Light scattering resonances in arbitrary-shaped one-dimensional reentrant surfaces

Pedro Negrete-Regagnon*[a], Rafael Hernández-Walls[a,b] and Victor Ruíz-Cortés[a]

[a] Centro de Investigación Científica y de Educación Superior de Ensenada
Apdo. Postal 2732, Ensenada, Baja California, 22800 México.

[b] Facultad de Ciencias Marinas, Universidad Autónoma de Baja California,
Apdo. Postal 453 Ensenada, Baja California, 22800 México.

ABSTRACT

Multiple scattering and shape-related effects are an active and important field of research in the area of diffraction and scattering of electromagnetic waves by rough surfaces. Most of the rigorous numerical techniques for dealing with this problem were limited to the treatment of single-valued surfaces. We have extended the formulation of Mendoza-Suárez and Méndez (1997) for dealing with multi-valued profile functions in order to study the scattering of reentrant surfaces or cavities in both, the near and far-field. We have evaluated the near-field in circular cavities with narrow entrances, as well as in the case of clusters of rods or cylinders. Resonant frequencies are clearly identified for these structures. We have also found that our model could be useful to predict wave-induced oscillations in harbors of arbitrary geometry. This comes from the fact that the mathematical formulation of the problem of light scattering by cavities (in the case of p polarization) is similar to the one employed in the case of harbors of arbitrary shape, when a water wave arrives at its entrance (Hwang and Tuck, 1970; Lee, 1971). The results obtained with our model are in close agreement with previously reported theories and experimental data.

Keywords: Surface scattering, morphology-dependent resonances, reentrant surfaces, near-field optics.

1. INTRODUCTION

In the last few years, there has been a significant advance in the study of scattering of electromagnetic waves by rough surfaces and particles. Partly motivated by the observation of enhanced backscattering[1,2] and other multiple scattering effects, rigorous numerical techniques to deal with problems of wave scattering from rough surfaces, have been developed.[3–7] Broadly speaking, one could divide the rigorous methods that describe the interaction of waves with rough surfaces into two main groups. Integral equation methods,[3–8] based on Green's integral theorem (or the extinction theorem), and differential methods.[9] The differential methods are better suited for surfaces with vertical walls, while the integral methods are more adequate for surfaces with gentle or moderate slopes.

Most rigorous numerical work on randomly rough surfaces is based on integral equation techniques. In its usual formulation, this method is limited to the treatment of surfaces whose profile can be described by single-valued functions. Few exceptions are known, as in the work by Moreno[10] and Valle,[11] where an extension for a particular case of a multi-valued surface profile is consider. They study the scattering of light by cylindrical (one-dimensional spherical) particles placed on a flat surface. Another technique that deals with simple reentrant cavities is described in the work by Skigin and Depine, based on a modal method, and consisting in expanding the field inside the cavity as a linear combination of its waveguide modes.[12]

In 1997, Mendoza-Suárez and Méndez[13] proposed a systematic approach for dealing with multi-valued profile functions. They parametrized analytically simple profiles and fractal surfaces, and calculated the electromagnetic field scattered by them. In this work we have applied their formulation to the study of the electromagnetic scattering by reentrant surfaces or cavities. The result is a technique valid for surfaces with rather arbitrary geometry and multiple profiles. Moreover, we can make use of the impedance boundary condition that allows us to eliminate two of the four unknown source functions, namely the electric and magnetic field and their derivatives.[14]

We have also found that our model could be useful to predict wave-induced oscillations in harbors of arbitrary geometry. This comes from the fact that the mathematical formulation of the problem of light scattering by cavities

*Correspondence: CICESE Optica, P.O. Box 434944, San Diego, CA 92143-4944, USA. Tel. 011-52-6-1744501, Fax: 011-52-6-1750553, e-mail: pnegrete@cicese.mx

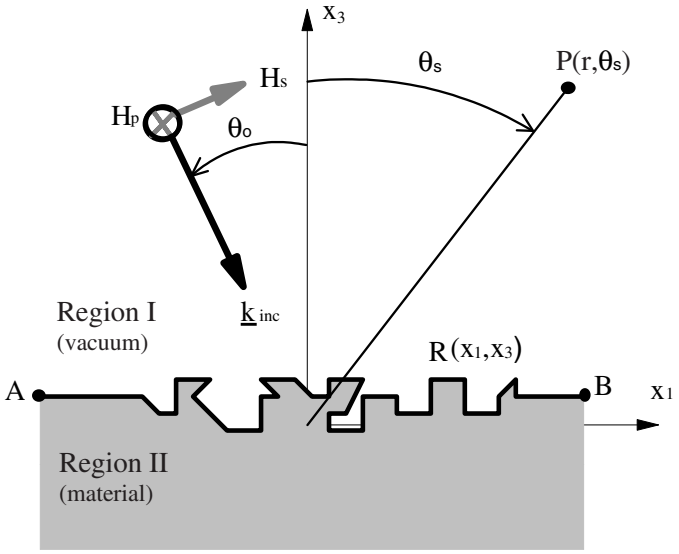

Figure 1. Geometry of the scattering problem. The surface profile $R(x_1, x_3)$ defines the boundary between regions I and II. Region I is vacuum, whereas region II is filled with a homogeneous and isotropic medium characterized by its complex dielectric constant $\epsilon(\omega)$. The surface is illuminated by a plane wave component with wave vector $\vec{k}_{inc}$. The angles of incidence and scattering are denoted by θ_0 and θ_s, respectively.

(in the case of p polarization) is similar to the one employed in the case of harbors of arbitrary shape, when a water wave arrives at its entrance. The results obtained with our model are in close agreement with previously reported theories and experimental data.[15,16]

The paper has been organized as follows: following closely the presentation of Ref. 3, but using a notation more appropriate for the present case, Sect. 2 presents the equations that determine the scattered fields and those required for the determination of the source functions. The emphasis of the present work is mainly in the numerical implementation of the method by Mendoza-Suárez and Méndez, leaving the mathematical details of the integral method to the references (see for instance Ref. 3). A description of the surface profile is given in Sect. 3, where we describe a procedure for numerically parametrizing an arbitrary profile in terms of the arc length of the curve (following Ref. 13). In Sect. 4 we describe the results obtained for the near-field oscillations in circular cavities with narrow entrances (10 and 60 degrees), as well as in the case of a cluster of rods or cylinders. The resonant frequencies are clearly identified for these structures. The possible application of this reentrant formulation for harbors and coastal bodies is briefly described in Sect. 5, where an example is presented. Finally, the concluding remarks are given in Sect. 6.

2. FORMULATION OF THE SCATTERING PROBLEM

In this section we will describe the physical situation considered. The scattering geometry is depicted in Fig. 1. The plane of incidence is the x_1x_3 plane, and the one-dimensional surface is illuminated by an electromagnetic wave of frequency ω and wave vector $\vec{k}_{inc}$. The angle of incidence is denoted by θ_0, and the angle of scattering by θ_s. The surface has height variations along the x_1 direction and is constant along the x_2 direction. The surface profile is represented by the continuous vector-valued function $\vec{R}(\xi, \eta)$, where (ξ, η) represent the coordinates of a point on the profile. Region I is vacuum, and region II is any isotropic medium, characterized by its frequency-dependent dielectric constant $\epsilon(\omega)$, or its complex refractive index $n_c = \sqrt{\epsilon(\omega)}$, with $\Re e\,[n_c(\omega)]$and $\Im m\,[n_c\,(\omega)] \geq 0$. For one-dimensional surfaces, when purely s or p polarized waves are incident on the surface, the state of polarization is not affected by interaction with the surface. Then the problem becomes essentially a scalar one and these two polarizations can be treated separately. We will consider only the case of p polarization and the material being a perfect conductor (although the use of a impedance boundary condition was implemented, for the sake of brevity it will not be described here). A comprehensive treatment for both polarizations is given elsewhere.[3,13]

According to the geometry, the magnetic field for the p polarization has the following form

$$\vec{H}(x_1, x_3) = [0, H(x_1, x_3), 0]\, e^{-i\omega t} \quad . \tag{1}$$

The x_2 component of the magnetic field in the vacuum, denoted by $H^I(x_1, x_3)$, satisfy the Helmholtz equation. Also this magnetic field satisfy the Neumann boundary condition

$$\hat{n}(\vec{R}) \cdot \frac{\partial}{dr} H^I(\vec{R}) = 0 \quad . \tag{2}$$

By applying the second Green's integral theorem in the vacuum region, and using the boundary condition, we obtain the total magnetic field as

$$H^I(\vec{r}) = H^I_{inc}(\vec{r}) + \frac{1}{4\pi} \int_{-\infty}^{+\infty} \left(\hat{n}(\vec{R}) \cdot \frac{\partial}{\partial \vec{r}} G^I(\vec{r}|\vec{R}) \right) H(\vec{R})\, ds \quad , \tag{3}$$

where $H_{inc}(\vec{r})$ represents the incident field, G^I is the Green function, $\vec{R}$ denotes the vector position given by the surface profile and $ds = \sqrt{d\overline{R} \cdot d\overline{R}}$ represent the differential of arc over the surface profile.

It should be clear that $H_{inc}(\vec{r})$ represent the incident field. The source function $H(\vec{R})$, on the other hand, is defined as

$$H(\vec{R}) = H^I(\vec{R}) \quad . \tag{4}$$

The source function $H(\vec{R})$ may be found from an integral equation obtained by letting the point of observation approach the surface. That is, we put $\vec{r} = \vec{R} + \upsilon \hat{n}(\vec{R})$, with υ a positive infinitesimal, and take the limit as $\upsilon \to 0_+$. We then have

$$H(\vec{R}) = H^I_{inc}(\vec{R}) + \lim_{\nu \to 0_+} \frac{1}{4\pi} \int_{-\infty}^{+\infty} \left(\hat{n}(\vec{R}) \cdot \frac{\partial}{\partial \vec{r}} G^I(\vec{R}' + \nu \hat{n}(\vec{R}')|\vec{R}) \right) H(\vec{R})\, ds \quad . \tag{5}$$

From this integral equation, the source function may be determined. The equation expressed by (3), on the other hand, give the total field at any point in region I in terms of the source function, and the term with the integral may be interpreted as the scattered field. Using a plane wave expansion for the Green's function, for observation points above the highest point of the surface, the field reflected into region I may be written as

$$H^I_{sc}(\vec{r}) = \frac{1}{2\pi} \int_{-\infty}^{\infty} R_p(k, \omega) e^{i\vec{Q} \cdot \vec{r}} dk \quad , \tag{6}$$

where the angular spectrum of the scattering field is:

$$R_p(k, \omega) = \frac{i}{2\alpha_o(k, \omega)} \int_{-\infty}^{\infty} \left[-i \left(\hat{n}(\vec{R}) \cdot \vec{Q} \right) H(\vec{R}) \right] e^{-i \frac{\omega}{c} \vec{r} \cdot \vec{R}} ds \quad , \tag{7}$$

where

$$\vec{Q} = (k, \alpha_0(kw)) \quad , \tag{8}$$

and

$$\alpha_0(k\omega) = \begin{cases} \sqrt{(\omega/c)^2 - k^2} & \text{if } k^2 < (\omega/c)^2 \,, \\ i\sqrt{k^2 - (\omega/c)^2} & \text{if } k^2 > (\omega/c)^2 \,. \end{cases} \tag{9}$$

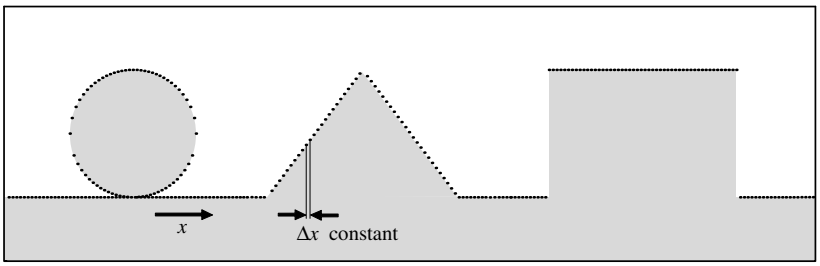

(a) Original surface, sampled at points [x,$\zeta(x)$]

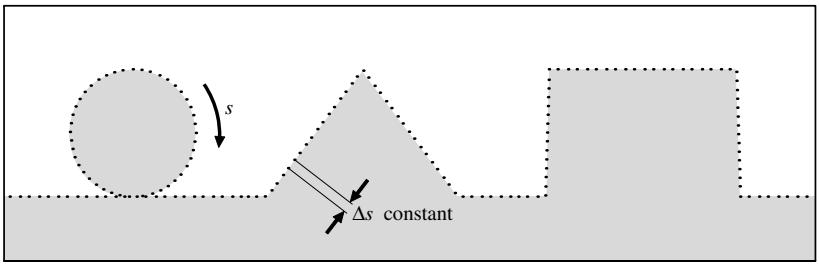

(b) Parametrized surface, sampled at points [$\xi(s)$,$\eta(s)$]

Figure 2. The formulation of the scattering problem in terms of a constant interval Δs is more adequate for sampling reentrant surfaces, specially those with large slopes.

2.1. Model for arbitrary one-dimensional profiles

The formulation of the scattering problem in terms of a parametrized profile is well suited for sampling reentrant surfaces, specially those with large slopes (see Fig. 2). In order to take into account such a reentrant profile, the equations developed previously for the scattered field need to be modified. This modification has been proposed by Mendoza-Suárez and Méndez,[13] and a brief summary of their procedure is given here.

We assume that the surface is of finite length, and that is represented by the curve Γ. Our basic aim is to describe the surface profile in terms of a parameter that can be conveniently chosen as the arc length along the Γ curve, so we can express the basic equations for the scattering of p-polarized waves in terms of this parameter.

First we need to establish all the necessary elements that must be satisfied by the reentrant surfaces. Once a reentrant surface profile comply these restrictions, we can assure the feasibility of parametrizing it and the existence of its first and second derivatives. Let the surface profile Γ be a rectifiable Jordan arc (p. 169 on Ref. 17) with a finite number of singular points (p. 315 on Ref. 17), and such that Γ is a directed path from point A to point B (see Fig. 1). With these conditions, it is possible to find a parameter t, such that the curve Γ can be described by a continuous single- and vector-valued function $\vec{R}$ of this parameter, defined in a closed interval. It is convenient in this case to choose the parameter t equal to the length of the curve s measured from A, the initial point of the curve. Note that if, for the case of profiles that can be described by a single-valued function of x_1, we choose x_1 as the parameter, we would reproduce the usual formulation of the problem. The profile of the surface can then be represented by the vector function $\vec{R}(s)$, such that the parametric interval, I_T, is $[0, L_T]$, where L_T represents the total length of the curve, i.e.,

$$L_T = \int_\Gamma ds \quad . \tag{10}$$

We assume in the following that the first and second derivatives of the function $\vec{R}(s)$ exist on each regular point of Γ. The scattering equations, on the other hand, are not well defined at the singular points of the curve Γ, and, to deal with this problem, we proceed as follows. Consider the M singular points on Γ (where M can be zero) given by the vectors $\vec{R}(s = L_1), \vec{R}(s = L_2), ..., \vec{R}(s = L_M)$. Having the M values of the parameter s where the singularities occur, we can divide the interval $[0, L_T]$ into $M + 1$ subintervals: $I_0 = [0, L_1), I_1 = (L_1, L_2), ..., I_1 = (L_M, L_T]$, so

that their union is a new parametric interval I'_T without singular points. We thus avoid the singular points in the integration process by using the interval I'_T. Although the function $\vec{R}(s)$ for the interval I'_T is not continuous, at least in principle this is not a problem, as it can be shown that the contribution that is due to the singular points is zero and the sources at the regular points are not affected by the existence of the singular points.[18] It is important to avoid, as we do, sampling at the singular points because one of the source functions is not defined there. It should also be noted that, because of the possibility of having strong variations of the field in the vicinity of the singular points, some difficulties in the numerical representation of the source functions in this vicinity may arise,constituting a possible source of cumulative errors. To proceed further, it is convenient to express the two components, (ξ, η), of the vector-valued function $\vec{R}(s)$, as functions of the parameter s. Then, at each regular point of the interval I'_T, we can write

$$\vec{R}(s) = [\xi(s), \eta(s)] \,. \tag{11}$$

The two parametric functions, $\xi(s)$ and $\eta(s)$, are of central importance to our formulation of the problem. We point out that, given a general profile that satisfies our assumptions, it is always possible to find, analytically or numerically, the functions $\xi(s)$ and $\eta(s)$, as well as their first and second derivatives on each point of the interval I'_T, starting from the relation

$$(ds)^2 = (d\xi)^2 + (d\eta)^2 \,. \tag{12}$$

At least formally, in each subinterval I_j, the functions $\xi(s)$ and $\eta(s)$ can be found by inversion of the functions $s(\xi)$ and $s(\eta)$, given by

$$s(\xi) = s(\xi_j) + \int_{\xi_j}^{\xi} \sqrt{1 + \left(\frac{d\eta(\xi)}{d\xi}\right)^2}\, d\xi \,, \tag{13}$$

and

$$s(\eta) = s(\eta_j) + \int_{\eta_j}^{\eta} \sqrt{1 + \left(\frac{d\xi(\eta)}{d\eta}\right)^2}\, d\eta \,, \tag{14}$$

where (ξ_j, η_j) are the coordinates of the point $\vec{R}(s = L_j)$ and $\eta(\xi)$ and $\xi(\eta)$ are functions that describe the surface profile in the interval explored by the variables of the line integrals. This provides a formal procedure for calculating the parametric functions $\xi(s)$ and $\eta(s)$ for each subinterval.

The normal and the normal derivative as functions of the parameter s are given by

$$n(\vec{R}) = (-\eta'(s), \xi'(s)) \tag{15}$$

and

$$\widehat{n} \cdot \frac{\partial}{\partial \overrightarrow{r}}|_{\overrightarrow{r}=\vec{R}} = \left(-\eta'(s)\frac{\partial}{\partial \xi(s)} + \xi'(s)\frac{\partial}{\partial \eta(s)}\right) \quad . \tag{16}$$

With these results, we can make further progress in the formulation of the scattering problem by writing Eq. (5) in terms of the functions $\xi(s)$ and $\eta(s)$,

$$\begin{aligned} H(s') \;=\; H(s')_{inc} \;+\; \lim_{\nu \to 0_+} \int_0^{L_T} \left[-\eta'(s)\tfrac{\partial}{\partial \xi(s)} + \xi'(s)\tfrac{\partial}{\partial \eta(s)}\right] \\ \times \; H_o^{(1)}\left(\tfrac{\omega}{c}\sqrt{\left(\xi'(s) - \xi(s) - \nu\eta'(s')\right)^2 + \left(\eta'(s) - \eta(s) - \nu\xi'(s')\right)^2}\right) H(s) ds \;, \end{aligned} \tag{17}$$

where we used the Hankel function of first class and zero order $H_o^{(1)}$ as a Green function that satisfy the Helmholtz equation for the given geometry.

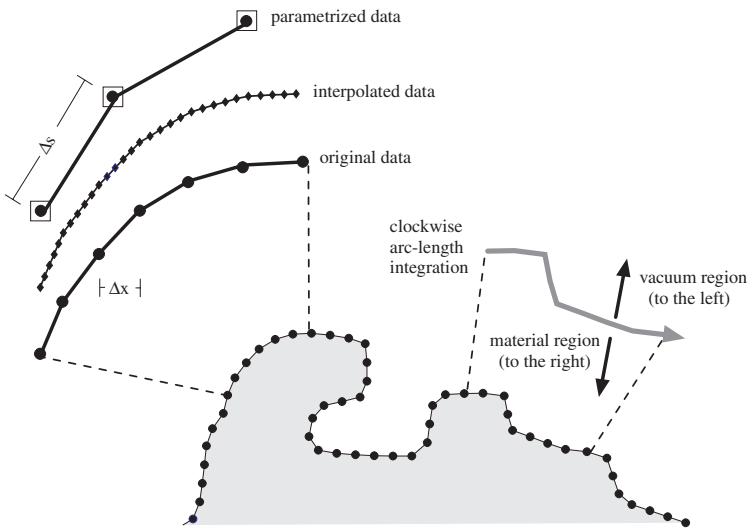

Figure 3. Numerical parametrization of the surface. The arc-length integration is carried out clockwise. By convention, the area located at the right of this direction corresponds to a region of material. The region to the left is vacuum.

3. NUMERICAL PARAMETRIZATION OF THE SURFACE

The work by Mendoza-Suárez and Méndez[13] describes the calculation for the electromagnetic field scattered by reentrant surfaces that were parametrized analytically. In the present work, we have extended their formulation in order to include arbitrary-shaped surfaces and also multiple profiles.

The surface parametrization described in the previous section has been carried numerically and is depicted in figure 3. In the case of a geometry consisting of several profiles, each one is treated (parametrized) independently. At the end we create an array comprising all the segments. We start the parametrization of each segment by choosing an initial point in the profile and by evaluating the arc-length along the surface in a clockwise direction. By convention, the part located at the right of this integration direction is consider to be inside the material. The area located to the left corresponds to vacuum.

For simplicity consider a profile given by a set of points (x, y) (this is equivalent to using coordinates (x_1, x_3) in Fig. 1). Starting at the initial point (x_1, y_1), we calculated the arc-length as the distance between this point an the following (x_2, y_2). If the calculated distance is less than a specified value Δs, we add to this quantity the distance obtained between points (x_2, y_2) and (x_3, y_3). In the case that this new distance exceeds the value of Δs, then the length between (x_2, y_2) and (x_3, y_3) is divided in segments of smaller length by means of a linear interpolation. These smaller segments are being added to the distance calculated previously until a close value to Δs is obtained (considering certain tolerance). The point obtained in this way becomes part of a the new array (x_s, y_s). From this point the calculation of the arc-length is reinitialized towards point (x_3, y_3). The parametrization consists then in obtaining the values (x_s, y_s) calculated from the original array (x, y) using the above described procedure.

Once the arrays (x_s, y_s) corresponding to each individual segment of the profile are obtained, we create a larger array containing all these elements, together with an array for their normal derivatives.

Once the surface profile has been parametrized, we need to define a grid of points (x_c, y_c) over which we need to evaluate the values for the scattered field. In a general way, these points do not correspond with the ones (x_s, y_s) over the profile, and we must employ an algorithm that allows us to discriminate if those points (x_c, y_c) belong to the region of material or to vacuum.

Our algorithm is based in the dot product and is illustrated in figure 4. For each element in the grid (x_c, y_c) we calculate the distance between this point and each of the points (x_s, y_s) in the surface profile. The smallest distance is then selected and a vector joining the points is created. This vector, called the minimum distance vector, has a direction that goes from point (x_c, y_c) towards point (x_s, y_s) and is almost perpendicular to the surface line (normal

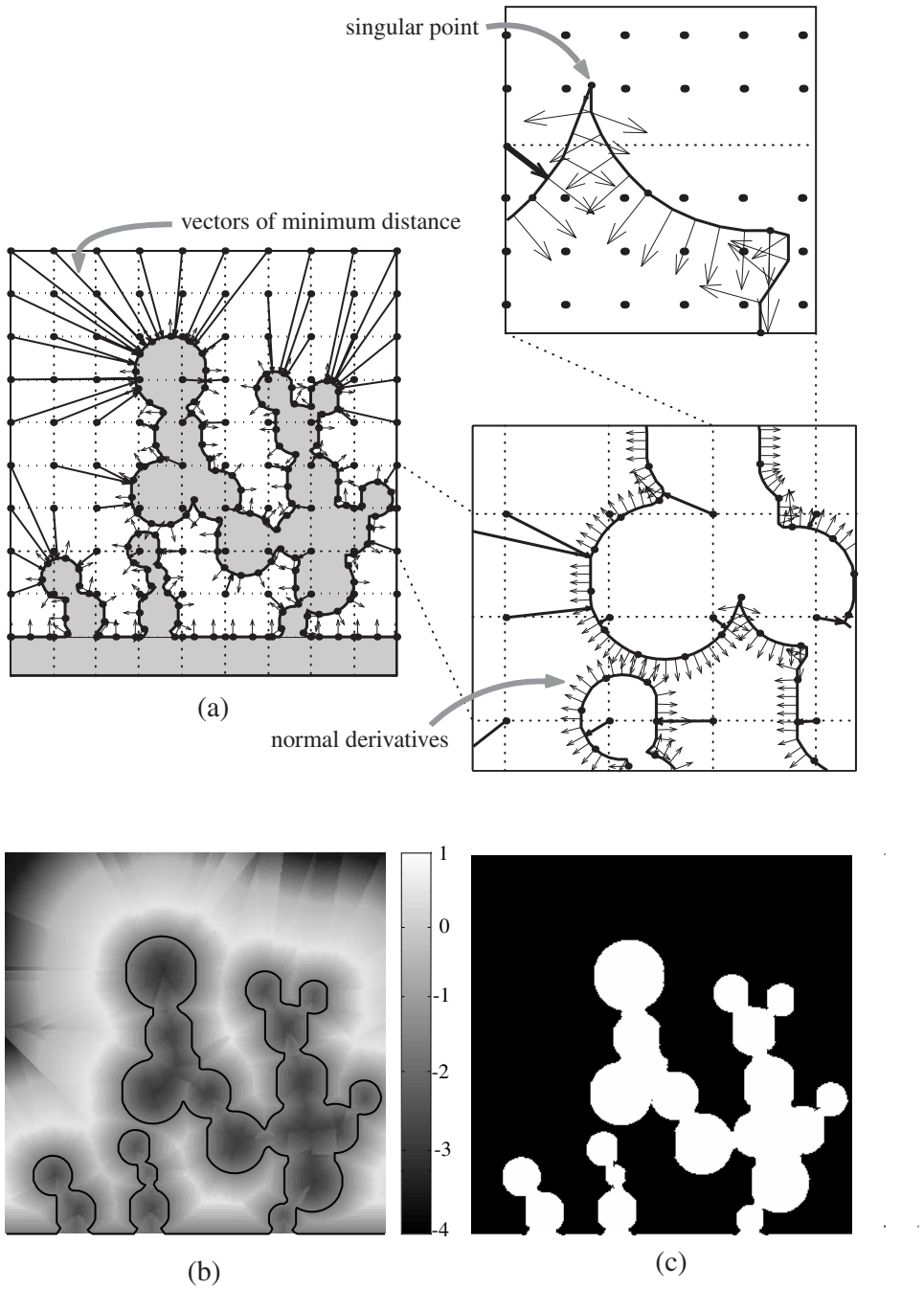

Figure 4. Algorithm based in the dot product used for selection of which points in a grid are located inside the material and which ones are contained outside. In (a) are illustrated the vectors of minimum distance coming form each point in the grid (x_c, y_c) and the normal derivatives to the surface (smaller arrows). It can be noted the presence of a singular point in the surface. This point can be identified because the magnitude of its normal derivative is considerably smaller than unity. According to the work by Mendoza-Suárez these singular points can be discarded with no effect in the field evaluation.[18] The dot product between the vector of minimum distance and the normal derivative, shown in (b), will be positive for those points inside of the surface. For those points located outside, the dot product will be negative. The output of the algorithm is illustrated in (c).

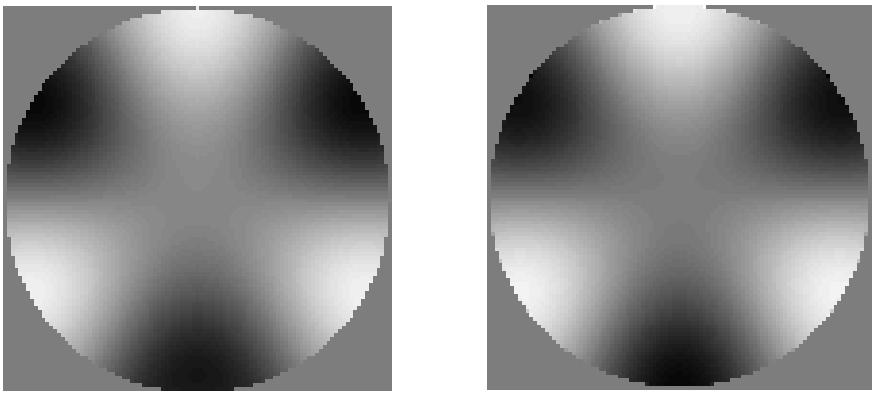

(a) Numerical solution (b) Analytical solution

Figure 5. Field oscillations inside a circular cavity with an aperture of 10 degrees. In (a) the calculation was performed using the reentrant formulation described in this work, whereas in (b) the field has been evaluated using an analytical solution.[19] The incident wavelength is equal to 1.4805 times the cavity radius and arrives from the top.

to the profile). In addition, we have vectors corresponding to the surface normal derivatives at each point (x_s, y_s). The dot product between the minimum distance vector and the normal derivative vector will be positive if both vectors points in the same direction, meaning that the point (x_c, y_c) is located inside the material region (see figure 4). On the other hand, the dot product will be negative when both vectors face each other, corresponding this to the case when (x_c, y_c) is located outside the surface.

4. RESULTS

The model for reentrant surfaces described previously was employed to evaluate the near-field scattered by simple cavities. We chose two circular cavities whose apertures correspond to 10 and 60 degrees. An analytical solution for the resonances in these cavities is known.[19] Figure 5 shows the case where the incident wavelength equals the radius of the cavity (for the 10 degree aperture). For the numerical parametrization we selected a Δs that corresponds to an arc-length of 0.5 degrees. The the numerical results are in good agreement with the analytical ones.

With the purpose of illustrating the near-field oscillations inside a cavity, figure 6 shows several images of the field calculated inside the 10 degree cavity as function of the incident wavelength for the case of p polarization. A clear difference regarding the use of a s-polarization incident wave can be appreciated in figure 7, where a similar sequence shows the field inside a cavity with a 60 degree aperture. Some oscillation modes in both figures can be easily identified.

A far more complex geometry is presented in figure 8. These results show some near-field calculation of light scattered by a cluster formed by cylindrical rods. In this particular case, it is possible to observe a dramatic enhancement in the magnitude of the field for a particular wavelength. For this experiment we observed an amplification factor (in amplitude) larger than 30 for a wavelength of 1.9725 microns.

5. APPLICATION TO ARBITRARY-SHAPE HARBORS

A harbor is a partially closed cavity connected with the ocean through one or more apertures. Resonant effect in harbors are of considerable importance and should be take into account during the design stage. The basic purpose of a harbor is to assure stability to the vessels located inside. Due to resonant effects, small-amplitude and low-frequency waves in open seas (a tsunami for instance), can produce enormous damage inside a harbor if an oscillation mode is excited.

Most of the existing work regarding modeling resonances in harbors and coastal bodies has been done using simple geometries.[19] In 1961, Miles and Munk studied resonant effect in harbors of constant deep by using a integral formulation, where the wave oscillations inside and outside the harbor were matched at the entrance. They obtained

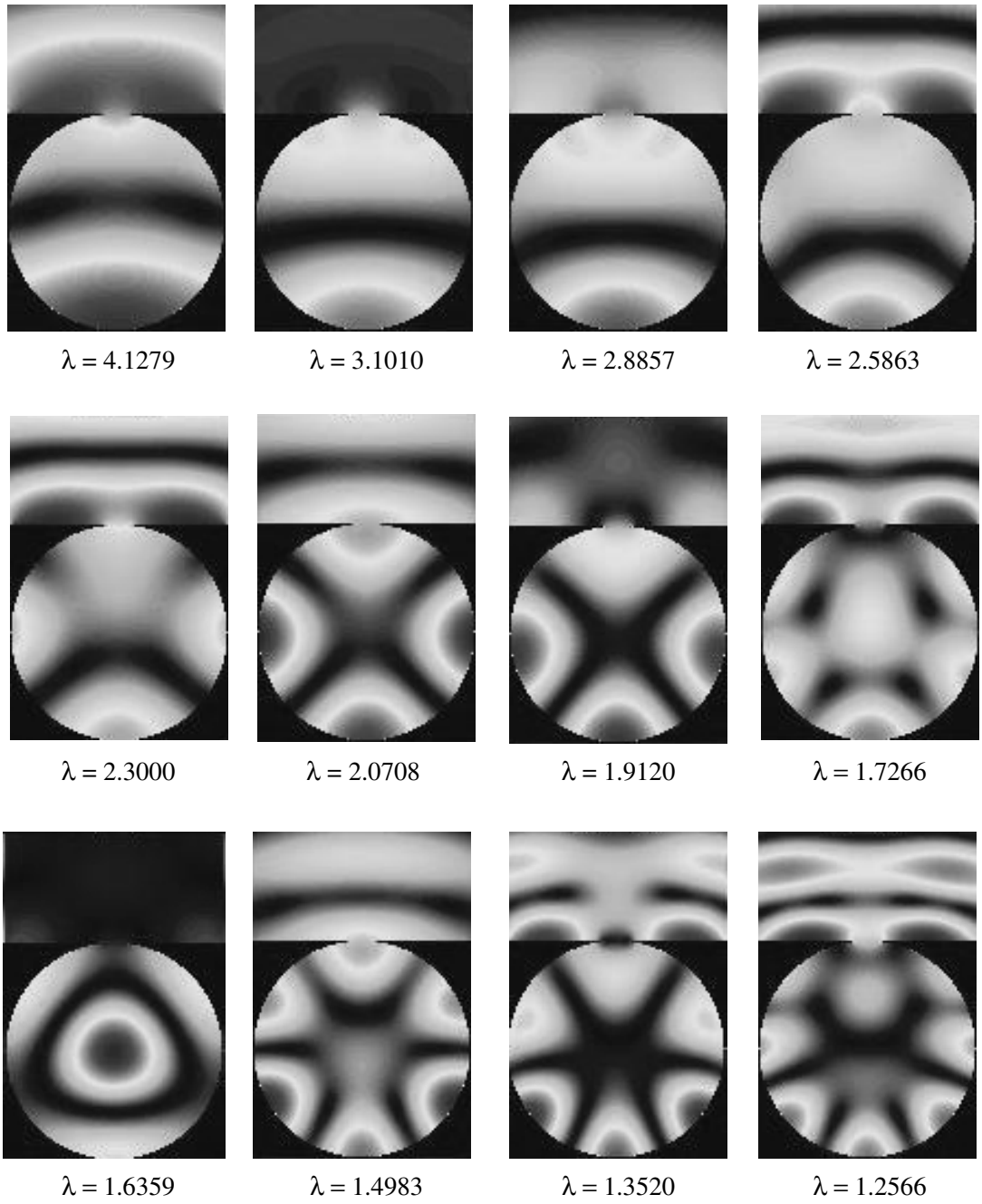

Figure 6. Sequence showing some near-field oscillation present in the 10 degrees-aperture cavity as a function of the wavelength. The incident unitary wave is p-polarized and arriving from the top. The cavity has a unitary radius. It should be noted that the bottom left image has a different gray scale for displaying purposes. The value of the resulting amplitude in the center of the cavity at that wavelength is larger than four.

an analytical model for rectangular harbors.[20] Ippend and Goda proposed, for the same geometry, a technique based in Fourier transformations.[21] They also obtained some experimental data that were in good agreement with their model. The use of an arbitrary geometry was originally proposed by Lee.[16] He developed a theory for harbors with constant deep, based on an integral method, resulting in a set of two coupled equations at the harbor entrance. Lee also obtained experimental data in water tanks for circular cavities that agree with his theory.

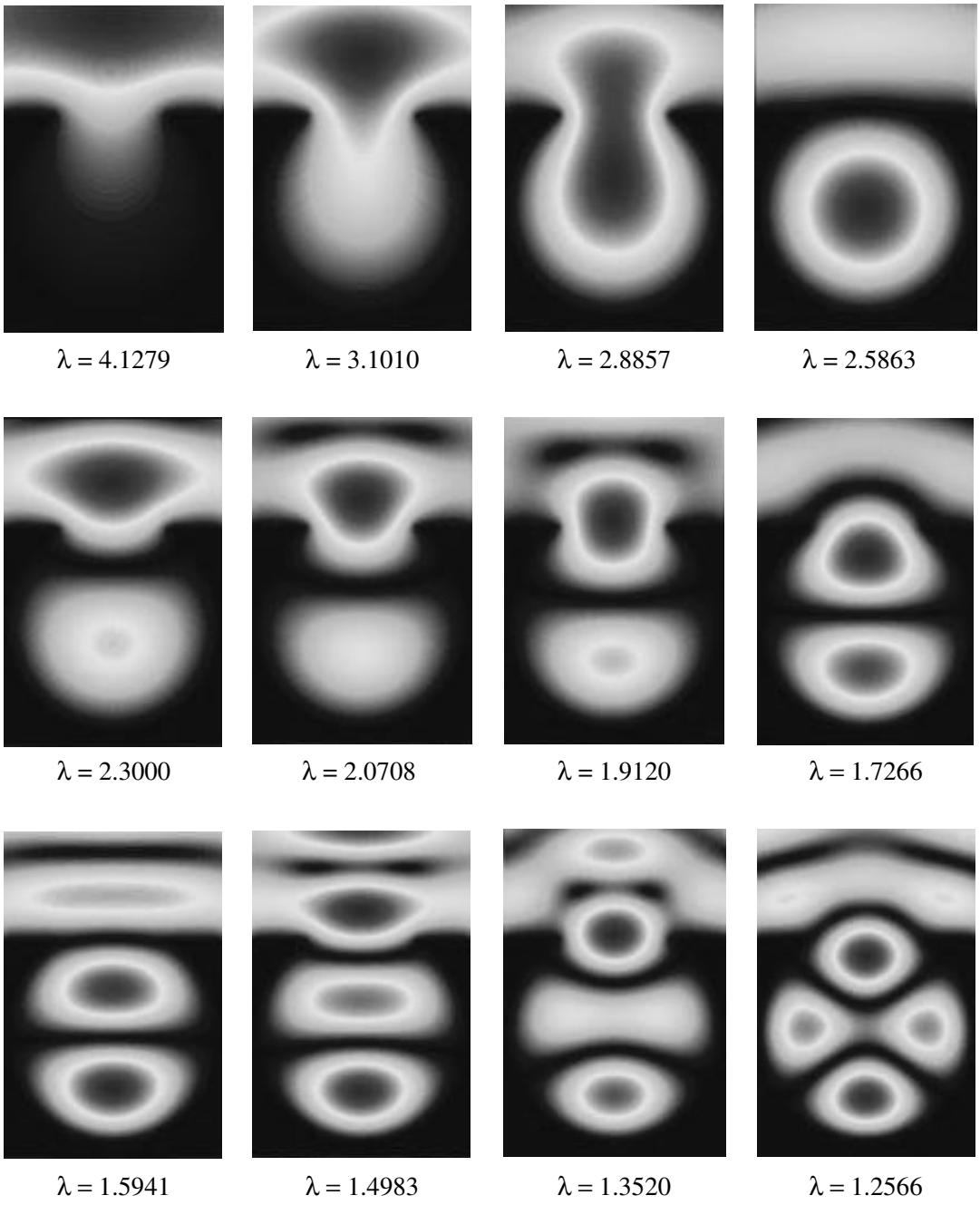

Figure 7. Sequence showing some near-field oscillation present in a 60 degrees-aperture cavity as a function of the wavelength. The incident unitary wave for this case is s-polarized and arriving from the top. The cavity again has unitary radius.

In this work we have found that the scattering model employed for reentrant surfaces, based in the integral equation and for p polarization, is also well suited for solving the problem of evaluating amplification factors inside arbitrary-shape and constant-deep harbors. Our current model resembles the one by Lee,[16] but there in no need of solving a set of coupled equations. The mathematical details that describe water waves oscillations in harbors are beyond the scope of this paper. A detailed manuscript is currently in the making. Here we will present only an example regarding the application of the reentrant formulation to study low-frequency wave oscillation in a coastal

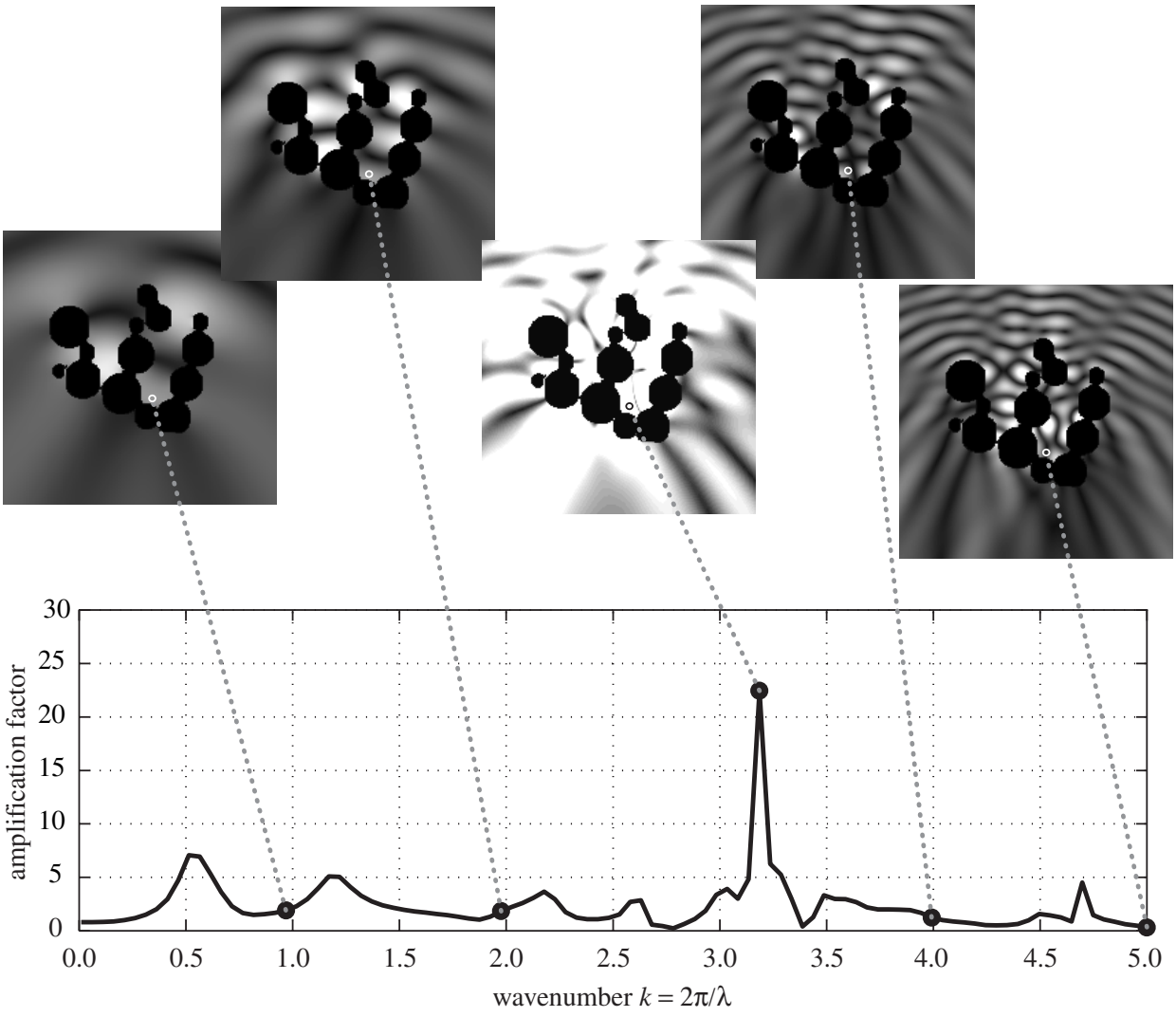

Figure 8. Sequence showing the near field scattered by a cluster of rods as functions of the wavelength. The incident p-polarized wave arrives form the top. Each image corresponds to an area of 10 by 10 microns. For this calculations we assumed a perfect conductor material for the scatterer. The amplification factor was measured in the point indicated by the dotted lines and represents how many times a unitary incident amplitude will be increased by morphology-dependent resonant effects.

body. Figure 9 shows the case of a one-dimensional cavity with the shape of the Ensenada bay (located in Baja California, México). The geometry consists of multiple profiles since the coast line includes also two islands. The image corresponds to an area or 10 by 10 units and shows the oscillations resulting from an incident wave of 1.4462 units arriving from the top. Results show amplification factors of almost five. The real area associated to the image is a square of approximately 25 kilometers by side. With such a scale, the incident wave of the above image should be 3.61 kilometers.

6. CONCLUDING REMARKS

This paper has been addressing the numerical implementation of the Mendoza-Suárez and Méndez model for evaluating the electromagnetic field scattered by arbitrary-shape reentrant surfaces.

We have obtained results for circular cavities that are similar to those obtained using an analytical solution. Also our results have been compared with experimental data, although in a different context, but resulting in a quite good

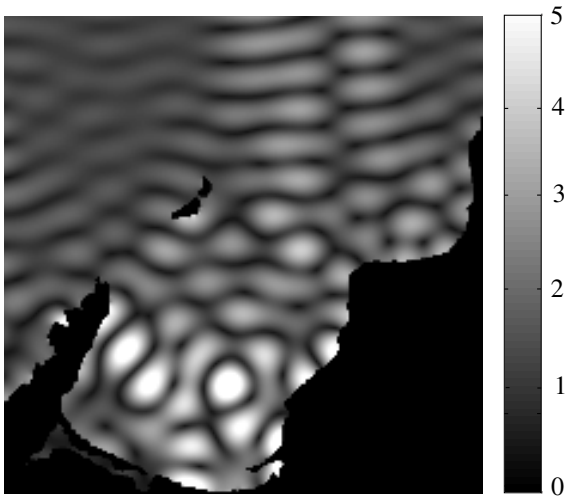

Figure 9. Example showing the application of the reentrant-surfaces scattering model to study wave-induced oscillations in harbors or coastal bodies of arbitrary geometry. We present the case of a one-dimensional cavity with the shape of the Ensenada bay (located in Baja California, México). The geometry consists of multiple profiles and has been parametrized in 894 points. The image corresponds to an area or 10 by 10 units and shows the oscillations resulting from an incident wave of 1.4462 units arriving from the top. Results show amplification factors of almost five. The real area associated to the image is a square of approximately 25 kilometers by side. With such a scale, the incident wave of the above image should be 3.61 kilometers.

agreement. This other context, the study of wave-induced oscillation in harbors and coastal bodies, has also been explored. We have found that the reentrant formulation for electromagnetic scattering in p polarization also solves the problem associated to arbitrary-shape oscillation in harbors due to the similarities in the mathematical models.

It can be said that the use of an impedance boundary condition in the scattering model can be employed to modeling the case of absorbing walls in harbors and partially reflecting coasts. This idea needs to be explored more deeply.

We have presented a clear example of a morphology-dependent resonance in a cluster of rods, where amplification factors of more than 30 have been observed in amplitude. Regarding this, the reentrant model can be of considerable help in study the implications of these field enhancements due to resonances associated to clusters and other complicated-shape geometries. This in the case of Raman scattering and several other non-linear optical effects.

ACKNOWLEDGMENTS

The authors thanks Adan Mejía-Trejo for letting them use his code for the evaluation of the analytical solution in the circular cavity. R. Hernández-Walls and P. Negrete-Regagnon are grateful to the Consejo Nacional de Ciencia y Tecnología (CONACYT) of México for financial support. Part of this work was supported by CONACYT grant I28147-E.

REFERENCES

1. E. R. Méndez and K. A. O'Donnell, ""Observation of depolarization and backscattering enhancement in light scattering from gaussian random surfaces"," *Opt. Commun* **61**, pp. 91–95, 1987.
2. K. A. O'Donnell and E. R. Méndez, ""Experimental study of scattering from characterized random surfaces"," *J. Opt. Soc. Am. A* **4**, pp. 1194–1205, 1987.
3. A. A. Maradudin, T. Michel, A. R. McGurn, and E. R. Méndez, "Enhanced backscattering of light from a random grating," *Ann. Phys. (N. Y.)* **203**, pp. 255–307, 1990.
4. E. I. Thorsos, "The validity of the kirchhoff approximation for rough surface scattering using a gaussian roughness spectrum," *J. Acoust. Soc. Am.* **83**, pp. 78–92, 1988.

5. D. Maystre, M. Saillard, and D. Maystre, "Scattering from metallic and dielectric rough surfaces," *J. Opt. Soc. Am. A* **7**, pp. 982–990, 1990.
6. B. J. Kachoyan and C. Macaskill, "Acoustic scattering from an arbitrary rough surface," *J. Acoust. Soc. A* **82**, pp. 1720–1726, 1987.
7. J. M. Soto-Crespo and M. Nieto-Vesperinas, "Electromagnetic scattering from very rough random surfaces and deep reflection gratings," *J. Opt. Soc. Am. A* **6**, pp. 367–384, 1989.
8. D. Maystre, *Electromagntetic Theory of Gratings*, Springer-Verlag, New York, 1980.
9. P. Vincent, *Electromagnetic Theory of Gratings*, Springer-Verlag, New York, 1980.
10. F. Moreno, F. González, J. M. Saiz, P. J. Valle, and D. L. Jordan, "Experimental study of copolarized ligth scattering by spherical metallic particles in conducting flat substrates," *J. Opt. Soc. Am. A* **10**, pp. 141–149, 1993.
11. P. J. Valle, F. González, and F. Moreno, ""Electromagnetic wave scattering from conducting cylindrical structures on flat surfaces: study by means of the extinction theorem"," *Appl. Opt.* **33**, pp. 512–523, 1994.
12. D. C. Skigin and R. A. Depine, "Modal method for scattering by arbitrarily shaped multivalued surfaces," *J. Mod. Opt* **45(9)**, pp. 1821–1843, 1988.
13. A. Mendoza-Suárez and E. R. Méndez, "Light scattering by a reentrant fractal surface," *Appl. Opt.* **36(15)**, pp. 3521–3531, 1997.
14. A. A. Maradudin and E. R. Méndez, "Theoretical studies of the enhanced backscattering of light from one-dimensional randomly rough metal surfaces by used of a nonlocal impedance boundary condition," *Physica A* **207**, pp. 302–316, 1994.
15. L. Hwang and E. O. Tuck, "On the oscillations of harbours of arbitrary shape," *J. Fluid Mech.* **42(3)**, pp. 447–464, 1970.
16. J. Lee, "Wave-induced oscillations in harbours of arbitrary geometry," *J. Fluid Mech.* **45(2)**, pp. 375–394, 1971.
17. T. M. Apostol, *Mathematical Analysis*, Addison-Wesley, New York, 1964.
18. A. Mendoza-Suárez, *Metodos rigurosos para el esparcimiento de luz por superficies y medios estratificados con perfiles arbitrarios*. PhD thesis, Centro de Investigación Científica y de Educación Superior de Ensenada, 1996.
19. C. Rodríguez-Pérez, *Análisis numérico de oscilaciones inducidas en la Bahía Todos Santos, B. C.*, Facultad de Ciencias Marinas, U.A.B.C., Tesis de Licenciatura, 1996.
20. J. W. Miles and M. Munk, "Harbour paradox," *Proc. Am. Soc. Civil Engineers* **WW3**(87), pp. 111–130, 1961.
21. A. T. Ippen and Y. Goda, *Wave induced oscillations in the harbours: Solution for a rectangular harbour connected to the sea*, M.I.T., Report No.59, 1963.